Eur. Phys. J. B **45**, 9–17 (2005)
DOI: 10.1140/epjb/e2005-00159-6

THE EUROPEAN PHYSICAL JOURNAL B

Spontaneous spin polarization in doped semiconductor quantum wells

L.O. Juri[a] and P.I. Tamborenea

Department of Physics "Juan José Giambiagi", University of Buenos Aires, Ciudad Universitaria, Pab. I, C1428EHA Buenos Aires, Argentina

Received 24 September 2004 / Received in final form 7 January 2005
Published online 16 June 2005 –

Abstract. We calculate the critical density of the zero-temperature, first-order ferromagnetic phase transition in n-doped GaAs/AlGaAs quantum wells. We predict that this transition could be observed in narrow quantum wells at electron densities somewhat lower than the ones that have been considered experimentally thus far, and that there exists an upper limit for the well width beyond which there would be no transition as long as only one subband is populated. Our calculations are done within a screened Hartree-Fock approximation with a polarization-dependent effective mass, which is adjusted to match the critical density predicted by Monte Carlo calculations for the strictly two-dimensional electron gas.

PACS. 73.21.Fg Quantum wells – 71.10.Ca Electron gas, Fermi gas – 71.45.Gm Exchange, correlation, dielectric and magnetic response functions, plasmons

1 Introduction

The interacting electron gas is one of the fundamental systems of physics. In spite of a long tradition of study, however, the subject still has many open basic questions. Notably, the issue of the existence of a ferromagnetic transition at low density has not been settled [1]. Coulomb correlations play a central role in the low-density regime, and taking them into account theoretically (i.e. going beyond Hartree-Fock) is unfortunately notoriously difficult. This problem has been most reliably tackled with numerically intensive Monte Carlo (MC) techniques [2–5]. For the two-dimensional jellium-model electron gas (2DEG), MC calculations indicate that, at $T = 0$, a first-order phase transition takes place at a certain critical value r_{sc} of the dimensionless average separation between electrons $r_s \equiv 1/\sqrt{\pi N_s} a_B^*$, where N_s is the surface density and a_B^* is the effective Bohr radius in the embedding medium ($a_B^* = 98.7$ Å for GaAs).

The most widely used methods in MC calculations [6] are the variational Monte Carlo (VMC), which predicts [2,3] a first-order phase transition at $r_{sc} = 13 \pm 2$ ($N_{sc} = 1.9 \times 10^9$ cm^{-2}), and fixed-node diffusion Monte Carlo (FN-DMC) with which $r_{sc} = 25$ ($N_{sc} = 5.2 \times 10^8$ cm^{-2}) has been found [4]. The VMC method uses a stochastic integration to evaluate the ground-state energy for a given trial wave function. The other method, which provides lower and more accurate ground-state energies, uses a projection technique to enhance the ground-state component of a trial wave function. In addition, in the FN-DMC method implemented in reference [4], backflow correlations [7] are included in the Slater determinant of the trial wave function, i.e. correlations are taken into account at the starting point of the process, for each polarization.

The strictly two-dimensional electron gas studied with MC techniques is an idealized theoretical model which has been introduced in order to describe in a simplified fashion experimentally available *quasi*-two-dimensional electron gases (quasi-2DEG), like the ones formed in negatively doped semiconductor quantum wells (QWs) [8–12]. By quasi-two-dimensional we mean here that the electronic wavefunction or the electronic density depend on the three usual coordinates, x, y, and z, but they are confined in one of the dimensions, say, z, to distances of the order of tens of nanometers, while in the other two dimensions the system size is macroscopic. The confinement in the z-direction gives rise to single-particle energy levels grouped in subbands [8–12]. In the systems we study here only one subband is populated due to the very low electron densities considered, but we still call our systems quasi-two-dimensional rather than *strictly* two dimensional because the electron slab has a finite width and its energy (as well as other properties, e.g., density profile, dipole moment for intersubband transitions, etc.), depends on this finite width, as well as on the particular form of the confining potential. Let us emphasize, then, that the strictly two-dimensional electron gas, which has zero width and no subband structure, and an electron gas confined in a quantum well with one-subband occupied are not identical systems, and in this paper we explore the differences that

[a] e-mail: luisjuri@jdcomp.com.ar

arise between the two regarding the state of spin polarization of the ground state. As a first example of the differences between both types of systems, we mention here the ground-state energies, equation (14) and equation (16), given in Section 2.1.

To the best of our knowledge, no Monte Carlo studies of the low-density phases of quasi-2DEGs comparable to the MC ones for uniform electron gases (in 2D and 3D) have been reported. This is due to the fact that the addition of the third spatial degree of freedom over which the electron gas is inhomogeneous increases prohibitively the computational cost of the calculations. We mention that the ferromagnetic transition in QWs has been studied theoretically in the frame of the local-spin-density approximation [13]. However, the critical densities predicted with that technique exceed by far the density interval given by MC for the 2DEG which makes them unreliable.

On the experimental front, the spin susceptibility has recently been measured in GaAs/AlGaAs superlattices [14], with electron densities as low as 1.7×10^9 cm^{-2}. In spite of the fact that this value falls into the density range predicted for a transition by the 2DEG-MC calculations, no transition was observed.

In this work, we study theoretically the possibility of a first-order transition at $T=0$ for the quasi-2DEG confined in GaAs/AlGaAs QWs as a function of the well width. Our goal is to make predictions for realistic semiconductor quantum wells that are at least consistent, as the zero-width limit is approached, with the benchmark predictions made with MC techniques for the uniform 2D jellium model electron gas. Our main finding is that the width and the depth of the well play a crucial role in the location (value of the critical density N_{sc}) and even the existence of the transition. In particular, we predict that there is an upper limit for the well width beyond which the ferromagnetic transition does not occur (always within the regime of only one subband occupied). We find that the transition could be observed at electron densities somewhat lower than those attained experimentally so far [14], for an optimum value of the well width, which we provide below. For our calculations we use a screened Hartree-Fock approximation scheme that includes a polarization-dependent effective mass which is introduced in order to take into account more accurately the effects of Coulomb correlation inside the well. This approach allows us to extend the results of the existing numerical Monte Carlo studies for the 2DEG to quasi-2DEG systems. Our formalism is explained in detail in this article, and our available evidence of its reliability when confronted with MC results is provided in Section 3.2 (see Fig. 3 and related text).

The paper is organized as follows. In Section 2.1 we introduce the basic scheme of the screened Hartree-Fock approximation and obtain the equations for the ground-state energies for the 2DEG and the quasi-2DEG. In Section 2.2 we present the results of this approximation and in Section 2.3 we analyze further those results and show that, according to our theory, an upper limit to the well width appears beyond which there is no transition. In Section 3 we describe the polarization-dependent effective-mass approximation and present and discuss the results obtained with it in combination with the available 2DEG Monte Carlo data. In Section 4 we discuss the experimental implications of our results and provide our recommendations for the observation of the ferromagnetic transition. We end in Section 5 with a summary of our conclusions.

2 Screened-Hartree-Fock theory with polarization-independent effective mass

2.1 Formalism

In a quasi-2DEG, the HF equation may be written as [15]

$$\left[E_n^{(\zeta)}(k)-\frac{\hbar^2k^2}{2m_b^*}\right]\Phi_{nk}^{(\zeta)}(z)= \left[-\frac{\hbar^2}{2m_b^*}\frac{d^2}{dz^2}+V_{ext}(z)+V_{sc}^{(\zeta)}(z)\right]\Phi_{nk}^{(\zeta)}(z) - \frac{2\pi e^2}{\varepsilon}\frac{1}{A}\int dz'\sum_{n'occup.}\sum_{|\mathbf{k}'|<k_{Fn'}^{(\zeta)}}\frac{e^{-|\mathbf{k}-\mathbf{k}'||z-z'|}}{|\mathbf{k}-\mathbf{k}'|} \times\Phi_{n'k'}^{(\zeta)*}(z')\Phi_{nk}^{(\zeta)}(z')\Phi_{n'k'}^{(\zeta)}(z), \quad (1)$$

where $\Phi_{nk}^{(\zeta)}(z)$ are the nth subband eigenstates and $E_n^{(\zeta)}(k)$ the corresponding eigenenergies, $m_b^*=0.067m_e$ is the effective mass (m_e being the electron rest mass), $\varepsilon=12.5$ is the dielectric constant, e is the electron charge, A is the crystal area, and $\mathbf{k}$ is the in-plane wave vector. In all our calculations we take the z-axis as the growth direction of the heterostructure. The self-consistent potential $V_{sc}^{(\zeta)}(z)$ is obtained by integration of the Poisson equation and is expressed as

$$V_{sc}^{(\zeta)}(z)=-\frac{4\pi e^2}{\varepsilon}\left(\int_0^z dz'(z-z')n^{(\zeta)}(z')-\frac{N_s}{2}z\right), \quad (2)$$

where the ζ-dependent electron density is

$$n^{(\zeta)}(z)=\frac{2-\zeta}{2\pi}\sum_{n\ occup.}\int_0^{k_{Fn}^{(\zeta)}}kdk|\Phi_n^{(\zeta)}(z,k)|^2. \quad (3)$$

Here, N_s is the doping sheet density and the external potential $V_{ext}(z)$ is the sum of the confinement potential of the heterostructure plus the electrostatic potential generated by the ionized donors (located symmetrically). The Fermi level $k_{Fn}^{(\zeta)}$ for each subband satisfies $2\pi(1+\zeta)N_s=\sum_n k_{Fn}^{(\zeta)2}$. We assume that the spin polarization index ζ only takes the values $\zeta=0$ and $\zeta=1$ since, at $T=0$, no stable partially-polarized phases have been found in 2DEG [4,16]. In contrast, recent calculations in 3DEG show that the transition is not of first order, but rather a continuous one involving partial spin-polarization states [5]. Here we make the hypothesis that the quasi-2DEG behaves like the 2DEG provided that the well width remains sufficiently small.

We solve equation (1) following a method similar to that developed in reference [15]. We expand the eigenfunctions $\Phi_{nk}^{(\zeta)}(z)$ in the single-electron QW-basis functions $\{\phi_n(z), \epsilon_n\}$, i.e.

$$\Phi_{nk}^{(\zeta)}(z) = \sum_p a_{pn}^{(\zeta)}(k)\phi_p(z). \tag{4}$$

This enables us to write the eigenvalue equation

$$\hat{H}^{(\zeta)}(k)\boldsymbol{b}_n^{(\zeta)}(k) = E_n^{(\zeta)}(k)\boldsymbol{b}_n^{(\zeta)}(k), \tag{5}$$

with $\boldsymbol{b}_n^{(\zeta)}(k) = (a_{1n}^{(\zeta)}(k), ..., a_{pn}^{(\zeta)}(k), ...)^T$. The matrix elements of the Hamiltonian operator $\hat{H}^{(\zeta)}(k)$ are

$$H_{tp}^{(\zeta)}(k) = \left[\epsilon_p + \frac{\hbar^2 k^2}{2m_b^*}\right]\delta_{tp} + \langle\phi_t|V_{sc}^{(\zeta)}|\phi_p\rangle - V_{tp}^{(1)(\zeta)}(k) - V_{tp}^{(2)(\zeta)}(k), \tag{6}$$

$$V_{tp}^{(1)(\zeta)}(k) = \frac{e^2}{\varepsilon}\sum_{n'}\int_0^{k_{Fn'}^{(\zeta)}} k'dk' \sum_{qr} G_{tr,qp}(k,k') \times a_{qn'}^{(\zeta)}(k')a_{rn'}^{(\zeta)}(k'), \tag{7}$$

$$V_{tp}^{(2)(\zeta)}(k) = \frac{e^2}{\varepsilon}\sum_{n'}\int_0^{k_{Fn'}^{(\zeta)}} k'dk' a_{pn'}^{(\zeta)}(k')a_{tn'}^{(\zeta)}(k') \times\frac{2}{\pi}\int_0^{\pi/2}\frac{d\varphi}{\sqrt{(k+k')^2 - 4kk'\sin^2\varphi + q_s^{(\zeta)}}}, \tag{8}$$

$$G_{tr,qp}(k,k') = \int\int dzdz'\phi_t^*(z)\phi_r(z)\phi_q^*(z')\phi_p(z') \times\int_0^{2\pi}\frac{d\varphi}{2\pi}\frac{e^{-|\mathbf{k}-\mathbf{k'}||z-z'|}-1}{|\mathbf{k}-\mathbf{k'}|}. \tag{9}$$

We note that equations from reference [15] have a number of misprints which are corrected here [17].

To introduce screening in the HF approximation we note from equations (7) and (8) that $V_{tp}^{(2)(\zeta)}(k)$ is the only term present in the pure 2D case and describes the long-range in-plane Coulomb interaction. Thus, we have dressed the interaction line of the exchange diagram [18] by replacing the bare Coulomb potential $V(q = |\mathbf{k}-\mathbf{k'}|) = (2\pi e^2/\varepsilon)(1/q)$ in equation (8) with the statically screened Coulomb potential

$$V_s^{(\zeta)}(q) = \frac{2\pi e^2}{\varepsilon}\frac{1}{q + q_s^{(\zeta)}}, \tag{10}$$

where $q_s^{(\zeta)} = (2-\zeta)/a_B^*$ is the ζ-dependent Thomas-Fermi wave number for the 2DEG. Unfortunately, the Fourier transform in 2D real space of equation (10) cannot be obtained analytically but its decay at large r is found to be [9]

$$V_s^{(\zeta)}(r) = \frac{e^2}{\varepsilon}\frac{1}{q_s^{2(\zeta)}r^3}. \tag{11}$$

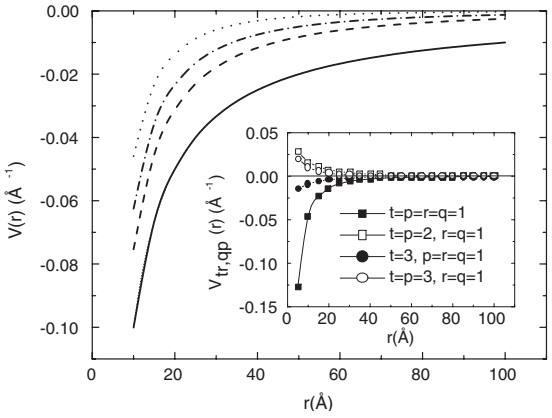

Fig. 1. Different Coulomb potentials. The solid line corresponds to the unscreened Coulomb potential $V(r) = 1/r$. The dashed (dot-dashed) curve corresponds to the Thomas-Fermi screened Coulomb potential for the polarized (unpolarized) case. The dotted curve represents the potential $V(r, d_W)$, Fourier transform of equation (9) (with respect to $q = |\mathbf{k}-\mathbf{k'}|$) for an infinite QW of $d_W = 100$ Å, for $t = r = q = p = 1$. Inset: the Fourier transform of equation (9) for an infinite QW of $d_W = 100$ Å for different values of t, r, q, p.

On the other hand, $V_{tp}^{(1)(\zeta)}(k)$ (Eq. (7)), which arises from the intrinsic inhomogeneity of charge distribution in the z-direction in a quasi-2DEG, represents an interaction of short range, and therefore is not affected significantly by screening. To see this, we consider the Fourier transform in 2D real space

$$V(r, |z-z'|) = \frac{e^2}{\varepsilon}\left(\frac{1}{\sqrt{r^2 + |z-z'|^2}} - \frac{1}{r}\right), \tag{12}$$

of the potential $V(q, z-z') = (2\pi e^2/\varepsilon)(e^{-q|z-z'|}-1)/q$ contained in equation (9). It can be shown that $V(r, |z-z'|)$ is of short range in the plane [10] and that at large r it can be approximated as

$$V(r, d_W) = -0.032\frac{e^2}{\varepsilon}\frac{d_W^2}{r^3}, \tag{13}$$

where we calculate the z and z' integration of $|z-z'|^2$ for an *infinite* QW of well width d_W setting the subband indexes equal to one. From equations (11) and (13) we note that both potentials decay at the same rate at large r and that $V(r, d_W) \approx 0.128V_s^{(0)}(r)$ and $V(r, d_W) \approx 0.032V_s^{(1)}(r)$ for $d_W = a_B^*$.

We show in Figure 1 that the potential defined by equation (12), suitably integrated over z and z' (dotted line), has a range that is shorter than the range of the Thomas-Fermi screened Coulomb potential for the polarized (dashed line) and unpolarized (dot-dashed line) cases, for $t = r = q = p = 1$. In the inset we show that this case

dominates over all others (we only show a few relevant examples). To summarize, we included static screening in $V_{tp}^{(2)(\zeta)}(k)$, equation (8), but not in $V_{tp}^{(1)(\zeta)}(k)$, equations (7, 9), for the reasons explained above.

In what follows we assume that only the first subband is occupied, and therefore the summations over the subband index may be omitted.

In solving the eigenvalue equation by iteration, we consider that self-consistency is achieved at the lth step if $|a_{pn}^{(\zeta)(l)}(k) - a_{pn}^{(\zeta)(l-1)}(k)|/|a_{pn}^{(\zeta)(l-1)}(k)| < 10^{-4}$ for all p, n and k. We obtain the set of eigenfunctions and eigenenergies $\{\Phi_{nk}^{(\zeta)}(z), E_n^{(\zeta)}(k)\}$ for $\zeta = 0$ and $\zeta = 1$, which allows us to write the ground-state energy per particle

$$E_{HF}^{(\zeta)} = \frac{2-\zeta}{4\pi N_s} \int_0^{k_F^{(\zeta)}} kdk \left[E_1^{(\zeta)}(k) + \tilde{\epsilon}_1^{(\zeta)}(k) + \frac{\hbar^2 k^2}{2m_b^*} \right], \tag{14}$$

with

$$\tilde{\epsilon}_1^{(\zeta)}(k) = \sum_n \epsilon_n |a_{n1}^{(\zeta)}(k)|^2. \tag{15}$$

In order to check our quasi-2DEG calculations in QWs when d_W tends to zero, we shall compare our results to the 2DEG screened HF case [19]

$$E_{HF2D}^{(\zeta)} = \frac{e^2}{2a_B^*\varepsilon} \left\{ \frac{1+\zeta}{r_s^2} - \frac{4}{\pi r_s}[2\zeta + \sqrt{2}(1-\zeta)]\mathbf{I}(x_\zeta) \right\}, \tag{16}$$

where $x_\zeta = \frac{1}{4}[\zeta + 2\sqrt{2}(1-\zeta)]r_s$ is the polarization-dependent Thomas-Fermi wave number divided by $2k_F^{(\zeta)}$ and

$$\mathbf{I}(x_\zeta) = \int_0^1 \frac{xdx}{x+x_\zeta} \left[\arccos(x) - x\sqrt{1-x^2} \right]. \tag{17}$$

2.2 Results

In this section we present the results obtained with the screened Hartree-Fock approximation with polarization-independent effective masses introduced in the previous Section.

In Figure 2, we plot the critical density for infinitely deep QWs (in which there is no barrier penetration) in the screened HF approximation as a function of well width d_W (solid squares). As expected, for densities lower than the critical density the polarized state is energetically favorable while the opposite is true for densities above the critical density. The limiting point at $d_W = 0$ (2DEG) was calculated with equation (16) and the remaining points with equation (14). The good match between these two different equations reflects the correctness of our derivations and calculations [17]. We note here that the critical density for the *infinite* QWs is a monotonically decreasing function of d_W. In the following section we will analyze in detail this effect.

We now use the previous result to analyze the critical density for *finite* QWs, plotted in Figure 2 with solid

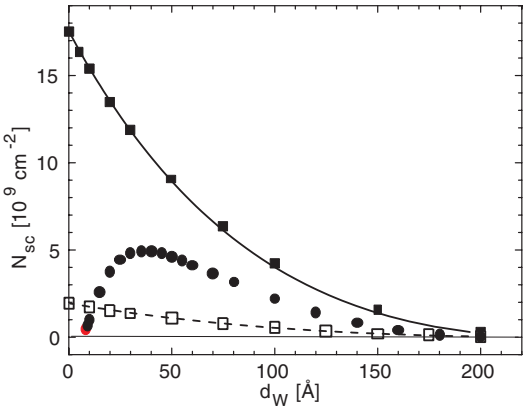

Fig. 2. Well-width dependence of the critical density in the screened HF approximation. Solid squares correspond to *infinite* quantum wells and solid circles to *finite* QWs with well height V_b=247 meV. Open squares correspond to *infinite* QWs with polarization-dependent effective masses with a constant ratio $f \equiv m_1^*/m_0^* = 0.65$. The solid and dashed lines are obtained with equations (24) and (27) (with $f = 0.65$), respectively, for *infinite* QWs.

circles. We set the height of the QWs to $V_b = 247$ meV, a typical experimental value [11]. This curve exhibits a non-monotonic dependence on the well-width showing a maximum for $d_W \approx 35$ Å. Also we observe a general reduction of the critical density with respect to the case of *infinite* QWs. This can be simply understood in terms of the previous result (monotonically decreasing critical density for the *infinite* wells) and the penetration of the electron wave function into the AlGaAs barriers; the latter causes the wave function to spread beyond the nominal well width, effectively "enlarging" the well. As a consequence, for example, a *finite* QW of $d_W \approx 60$ Å has the same critical density as that of an *infinite* QW of $d_W \approx 100$ Å. In fact, the penetration depth $d_B = \hbar/\sqrt{2m_b^*(V_b - E_1)}$ increases when E_1 is raised as d_W is lowered [10]. This effect produces an inflection point at $d_W \approx 75$ Å and the mentioned maximum at $d_W \approx 35$ Å due to the competition between d_W and d_B.

Let us go back to the curve for *infinite* QWs in Figure 2. The limiting ($d_W = 0$) value $N_{sc} = 17.5 \times 10^9$ cm^{-2} corresponds to $r_{sc} = 4.32$, showing a sizable increase with respect to the (unscreened) HF value $r_{sc} = 2.01$ [20]. This increase, however, is not sufficient if we consider the value $r_{sc} = 13$ obtained in reference [2] using VMC. This indicates that a significant degree of Coulomb correlation is being left out in the screened HF approximation. In Section 3 we come back to this problem.

2.3 Analysis: upper limit for the well width

We noted in the previous section that the critical density for the *infinite* QWs is a monotonically decreasing function of d_W (Fig. 2). This result can be understood within our screened HF scheme in terms of the interplay between different components of the exchange interaction in a quasi-2DEG. In this section we analyze in detail this

issue. As an aid to the reader, we mention that the following analysis is somewhat technical, but we choose to include it here since from it we also derive an important result of this paper, namely, that there exists an upper limit for the well width beyond which the ferromagnetic transition does not take place (assuming that only one subband is occupied). Therefore, the reader may skim through the following paragraphs or go directly to the paragraph of the interesting equation (25).

We found that the coefficients $a_{p1}^{(\zeta)}(k)$ (Eq. (4)) change very little with k and $a_{11}^{(\zeta)}(k) \approx 1$ whereas $a_{p1}^{(\zeta)}(k) \ll 1$ for $p > 1$. This result is a direct consequence of the small-density condition since, if this condition is met, the ground-state wave function must retain the shape of its one-electron counterpart in a QW. Thus, $V_{11}^{(2)(\zeta)}(k)$ (Eq. (8)) is positive and it is the leading matrix element, yielding a negative (see Eq. (6)) and d_W-independent contribution to the exchange energy (pure 2D case). In contrast, the matrix elements $V_{tp}^{(1)(\zeta)}(k)$ are slowly varying functions of k since we are studying small-width and low-density heterostructures. If these conditions are fulfilled, we can expand the exponential in equation (9) up to first order since the exponent satisfies the following inequality:

$$|\mathbf{k}-\mathbf{k'}||z-z'| \leq 2k_F^{(\zeta)}d_W = 2\sqrt{2(1+\zeta)}\frac{1}{r_s}\frac{d_W}{a_B^*} \leq 0.3, \tag{18}$$

provided that $r_s \geq 13$ (lower MC limit for the transition) and the well width $d_W \leq a_B^*$ (= 98.7 Å). Then we perform the integration over z and z' (*infinite* QWs) yielding $G_{11,11} = -0.207 d_W$. Thus, $V_{11}^{(1)(\zeta)}$ is negative, proportional to d_W and k-independent. The matrix elements $V_{tp}^{(1)(\zeta)}$ for indices with opposite parity are always zero since due to the symmetry of the wave functions we have $G_{t1,1p} = 0$. On the other hand, we have evaluated $G_{t1,1p}$ for indices with equal parity obtaining that these are considerably smaller than $G_{11,11}$ rendering $V_{tp}^{(1)(\zeta)}$ practically diagonal. Also, $\langle\phi_t|V_{sc}^{(\zeta)}|\phi_p\rangle \approx 0$ (see Eq. (6)) for the non-diagonal elements since, due to the low-density condition, $V_{sc}^{(\zeta)}$ must be a very slowly varying function of z. Thus, $H_{tp}^{(\zeta)}(k)$ is almost diagonal, being its first eigenenergy

$$E_1^{(\zeta)}(k) \approx \epsilon_1 + \frac{\hbar^2 k^2}{2m_b^*} + \langle\phi_1|V_{sc}^{(\zeta)}|\phi_1\rangle - V_{11}^{(1)(\zeta)} - V_{11}^{(2)(\zeta)}(k). \tag{19}$$

With this expression for $E_1^{(\zeta)}(k)$ we can obtain an approximate equation for N_{sc}. We only need to make two easily justified additional approximations. From the behavior of the coefficients $a_{p1}^{(\zeta)}(k)$, i.e. $a_{11}^{(1)}(k) \approx a_{11}^{(0)}(k) \approx 1$ and $a_{p1}^{(1)}(k) \approx a_{p1}^{(0)}(k) \approx 0$ for $p > 1$ it can be seen (from Eq. (15)) that $\tilde{\epsilon}_1^{(\zeta)}(k) \approx \epsilon_1$ and (from Eq. (4)) $\Phi_{1k}^{(\zeta)}(z) \approx \phi_1(z)$. Using the latter in equation (3) we get $n^{(\zeta)}(z) \approx (2-\zeta)(1+\zeta)N_s\phi_1^2(z)/2 = N_s\phi_1^2(z)$, and therefore a ζ-independent $\langle\phi_1|V_{sc}|\phi_1\rangle$ (see Eq. (2)). By inserting equation (19) in equation (14) we obtain, after some algebra, the following equation for the energy shift between both phases

$$E_{HF}^{(1)} - E_{HF}^{(0)} \approx \frac{\pi N_s e^2 a_B^*}{2\varepsilon}\left[1 + 0.207\frac{d_W}{a_B^*} - 4F(N_s)\right], \tag{20}$$

where

$$F(N_{sc}) = \int_0^1 x dx \int_0^1 x' dx' \times \frac{2}{\pi}\int_0^{\pi/2} d\varphi [g_1(N_{sc},x,x',\varphi) - g_0(N_{sc},x,x',\varphi)], \tag{21}$$

with

$$g_0(N_{sc},x,x',\varphi) = \left[\sqrt{2\pi N_{sc}}a_B^* \times\sqrt{(x+x')^2 - 4xx'\sin^2\varphi} + 2\right]^{-1}, \tag{22}$$

and

$$g_1(N_{sc},x,x',\varphi) = \left[\sqrt{\pi N_{sc}}a_B^* \times\sqrt{(x+x')^2 - 4xx'\sin^2\varphi} + q_s^{(1)}/q_s^{(0)}\right]^{-1}, \tag{23}$$

where $x \equiv k/k_F^{(0)}$ in g_0 and $x \equiv k/k_F^{(1)}$ in g_1. The same holds for x' and k'.

Taking into account that the energy shift $E_{HF}^{(1)} - E_{HF}^{(0)}$ must be zero at the transition density, we may write the following equation that relates d_W and N_{sc}

$$1 + 0.207\frac{d_W}{a_B^*} = 4F(N_{sc}). \tag{24}$$

Finally, to demonstrate that the transition density is a decreasing function of the well width, we need to prove that $F(N_{sc})$ is also a decreasing function. To see this, we note firstly that $g_1 > g_0$ for all values of its arguments making the function $F(N_{sc})$ always positive allowing equation (24) to be solvable. Secondly, both g_0 and g_1 are decreasing functions of N_{sc} for all values of x, x', φ and it is straightforward to prove that g_1 decreases more rapidly than g_0 making $F(N_{sc})$ a decreasing function. Thus, an increase of d_W must be accompanied with a decrease of N_{sc} proving that the monotonically decreasing dependence of N_{sc} on d_W is governed by the competing action of the different components of the exchange interaction: the in-plane component represented by $F(N_{sc})$ and the out-of-plane term driven by d_W. The behavior of g_0, g_1 and F that we described can also be recognized in the unscreened HF case indicating that the dependence of N_{sc} on d_W is purely due to exchange. The validity of our approximation can be verified in Figure 2 where the solutions of equation (24) are depicted with the solid line. This curve approaches very well the exact values (solid squares) indicating that the approximations we made to derive it are well justified. For low densities (high r_s) and low well

widths, the solid curve fits excellently the solid squares since in these regimes the approximations we made become exact. In the intermediate region ($d_W \approx 100$ Å) the solid curve fits very well the solid squares.

A look at equation (24) also indicates that there exists an upper limit for the well width beyond which there is no transition. In fact, due to the decrease of $F(N_{sc})$ and since $F(0)$ is finite, it can be seen from equations (22) and (23) that the following relation holds

$$0.207\frac{d_{WL}}{a_B^*} = \frac{q_s^{(0)}}{q_s^{(1)}} - \frac{3}{2}. \tag{25}$$

Thus, it must be $d_W < d_{WL} = 2.42a_B^* \approx 239$ Å to allow the confined electrons to reach the polarized phase. This new result is entirely due to the Thomas-Fermi screening and is not present in the unscreened HF approximation since $F(0)$ diverges in this case. Furthermore, the ratio of the Thomas-Fermi wave numbers for both polarizations must be $q_s^{(0)}/q_s^{(1)} > 3/2$ (in our case it is $q_s^{(0)}/q_s^{(1)} = 2$). Otherwise, no polarized state could be possible in a QW. These key results indicate that the well width plays a crucial role in the search for spontaneous spin polarization in QWs [21].

The implications of the existence, according to our calculations, of an upper limit for the well width must be considered with some care. If one attempts to reach a 3DEG system by increasing the well width one would apparently fall into the paradox that no transition is possible in 3DEG. This conclusion is incorrect for two reasons. First, we must take into account that the 3DEG-MC results are obtained in the jellium model, in which the positive background is taken to be a uniform neutralizing static charge distribution, whereas in our quantum-well calculations the positive charges of the ionized donors are located far away from the electron gas, which results in an important change in the direct Coulomb energy. In other words, wide-enough quantum wells and 3DEG jellium model must be considered as different systems. Secondly, our calculation assumes that only one subband is occupied (a valid assumption in narrow quantum wells at low density) whereas any extrapolation of our conclusions to 3DEG systems would have to contemplate necessarily occupation of many subbands. Thus, we reach the conclusion that the most likely scenario is that there is a phase transition in narrow quantum wells, which disappears for intermediate well widths, and reenters at wider well widths as expected when the 3DEG limit is approached.

3 Polarization-dependent effective masses

3.1 Motivation

In order to improve our treatment of Coulomb correlation, we need an approximation scheme applicable to the quasi-2DEG such that as d_W tends to zero (strictly 2D electron gas) the critical density approaches the values predicted by MC calculations [2–4]. To achieve this, we incorporate phenomenological polarization-dependent effective masses m_0^* (unpolarized) and m_1^* (polarized) in our formalism. Due to the lack of experimental data on effective masses in GaAs/AlGaAs heterostructures for both polarizations and to the fact that no calculations on polarized effective masses exist in 2DEG, we resort to calculations of unpolarized effective masses and ground-state energies in pure 2DEG [2,22,23] to justify this procedure. Let us summarize the conclusions of those studies relevant in our context:

(a) Coulomb correlation increases the effective mass [23].
(b) The absolute value of the correlation energy of the unpolarized 2DEG ground state is greater than its polarized counterpart [2].
(c) The absolute value of the correlation energy is greater in 2D than in 3D (both unpolarized), leading to 2D effective masses substantially larger than those of the 3D case at equal r_s [22].
(d) The correlation-energy shift between both phases in 2D is greater than the unpolarized correlation energy shift between 2D and 3D [2].

Making use of (a) and (b), with the supporting evidence of (c) and (d), we conclude that *m_0^* must be substantially larger than m_1^* at equal r_s*. Therefore, we will introduce the ratio $f = m_1^*/m_0^*$ and use it as an adjustable parameter. We will find that it needs to be assigned values $f < 1$, as expected, in order to match the screened HF to the MC calculations.

3.2 Two-dimensional case

By defining the ratio $f = m_1^*/m_0^*$ and rewriting $x_\zeta = \frac{1}{4}[f\zeta + 2\sqrt{2}(1-\zeta)]r_s$ we may generalize equation (16) for the 2DEG:

$$E_{HF2D}^{(\zeta)} = \frac{e^2 m_0^*}{2a_B^*\varepsilon}\left\{\frac{1+\zeta}{[(f-1)\zeta+1]r_s^2} - \frac{4}{\pi r_s}[2\zeta + \sqrt{2}(1-\zeta)]\mathbf{I}(x_\zeta)\right\}. \tag{26}$$

We observe from reference [22] that $m_0^* \approx 1.2$ for $r_s > 5$ in the modified Hubbard approximation. That approximation is an attempt at including correlation effects by means of the introduction of the Thomas-Fermi wave number in the so-called local-field correction factor. Since we have incorporated screening correlations and HF effects within a similar scheme, we take $m_0^* = 1$ in equation (26) to avoid an overestimation of the effective mass in the unpolarized phase.

Using equation (26), the lowest 2DEG-VMC value, i.e. $r_{sc} = 13$, is obtained with $f = 0.65$. With this value of f we calculate $E_{shift} = E_{HF2D}^{(1)} - E_{HF2D}^{(0)}$ and plot it versus r_s in Figure 3 (solid line). Here we have taken $e^2/2a_B^*\varepsilon = 1$ Ry to compare our E_{shift} to MC results. The solid circles correspond to the results obtained in reference [2] and the open squares are from reference [3]. We note the excellent agreement between our curve and the MC points: by

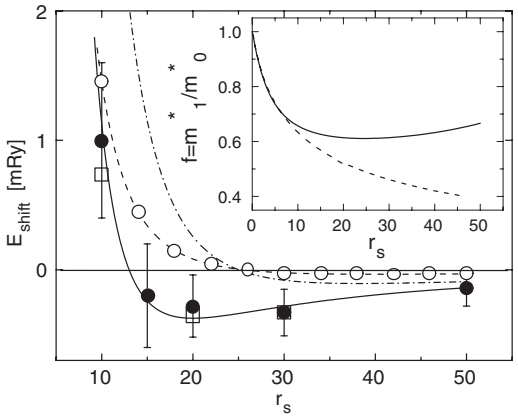

Fig. 3. Ground-state energy shift for the 2DEG $E_{shift} = E^{(1)}_{HF2D} - E^{(0)}_{HF2D}$ versus r_s. Solid circles represent the reported values in Table I of reference [2]. The error bars denote the VMC standard errors. Open squares correspond to the values tabulated in Tables I and II for the VMC method in reference [3]. No error bars are plotted for clarity. Open circles are from reference [4]. The solid and dot-dashed lines represent our calculations obtained with equation (26) for polarization-dependent effective masses using $f = 0.65$ and $f = 0.49$ respectively. The dashed curve corresponds to the same calculations but using the values of f that come from $f(r_s)$ showed in the inset (dashed line). In the inset, solid and dashed lines correspond to the values of f that fit the curves E_{shift} from reference [2] and reference [4] respectively.

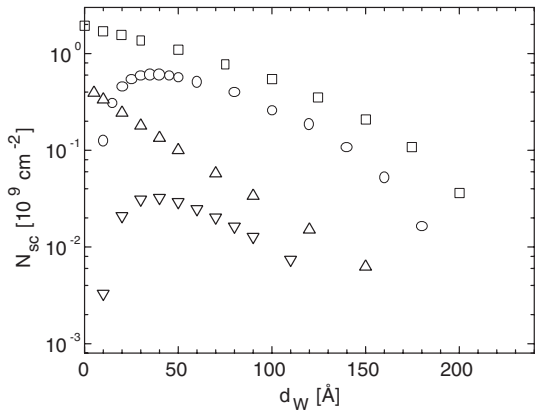

Fig. 4. Well-width dependence of the critical density in the screened HF approximation with polarization-dependent effective masses. Open squares (circles) correspond to *infinite* (*finite*) QWs with a constant ratio $f \equiv m^*_1/m^*_0 = 0.65$. Up (down) triangles correspond to *infinite* (*finite*) QWs for a ratio f which depends on r_s (dashed line in the inset of Fig. 3).

adjusting only one point our curve meets all the points obtained in references [2,3]. In other words, our "screened HF plus $f < 1$" scheme agrees with VMC [2,3] for a constant (density independent) value of f. This agreement indicates that, according to VMC, the ratio between both effective masses would depend weakly on the density. This conclusion is consistent with the fact that in the modified Hubbard approximation the unpolarized effective mass is a slowly varying function for $r_s > 5$ [22]. If this were also the behavior of the polarized effective mass, we could conclude that f would be a slowly varying function of r_s.

We now repeat the previous analysis but using the FN-DMC data of Attaccalite et al. [4]. In that paper the authors obtain $r_{sc} = 25$ which, as we mentioned in the introduction, is the highest value found in the literature for spontaneous spin polarization in 2DEG at zero temperature. We find that equation (26) reproduces the value $r_{sc} = 25$ when $f = 0.49$. In Figure 3 (dash-dotted line) we plot the energy shift, $E_{shift} = E^{(1)}_{HF2D} - E^{(0)}_{HF2D}$, versus r_s, for this value of f. This curve does not fit well the data from reference [4] shown as open circles. Instead, we find that equation (26) can reproduce (dashed line in Fig. 3) the FN-DMC energy shifts [4] if f is considered a function of r_s (dashed line in the inset). Therefore, we conclude that FN-DMC appears to support the idea of a density-dependent ratio of the effective masses.

For completeness, we show in the inset (solid line) the values of f as a function of r_s that fit the parametrization of E_{shift} obtained by Ceperley [2]. This curve exhibits a weak dependence on r_s for $r_s > 10$, which explains the good agreement with VMC we obtained with a constant value $f = 0.65$, seen in Figure 3 (solid line and symbols).

3.3 Quasi-two-dimensional case

We now apply the polarization-dependent effective-mass approximation to the quasi-2DEG by means of a slight modification in equation (1). We note that the two effective masses m^*_b on both sides of equation (1) belong to different situations [10]: the m^*_b on the l.h.s. represents the in-plane effective mass and therefore is being affected by Coulomb correlations. In contrast, the m^*_b on the r.h.s. reflects the out-of-plane effective mass of one electron moving in the z-direction governed mainly by $V_{ext}(z)$ and $V^{(\zeta)}_{sc}(z)$, and thus not being affected by Coulomb correlations, according to our discussion about screening in Section 2.1. Then we solve the eigenvalue equation, equation (1), and use equation (14) for both polarizations incorporating the effective masses $m^*_0 = m^*_b$ and $m^*_1 = f m^*_b$ (the last one only in the in-plane terms). We plot in Figure 2, with open squares, the results obtained for *infinite* QWs for $f = 0.65$. We calculate the limiting point at $d_W = 0$ with equation (26) and the remaining points with equation (14) with the above-mentioned replacement. We obtain again a good match between both calculations, analogously to what happens with the solid squares ($f = 1$ calculations). We show in Figure 4, in a logarithmic scale for the vertical axis, the results for *finite* QWs (open circles) and *infinite* QWs (open squares) where we have taken $f = 0.65$. Both curves exhibit the same general characteristics as in Figure 2 (solid squares and solid circles).

Now we obtain an equivalent of equation (24) by incorporating the ratio f that multiplies the band mass m^*_b for the polarized phase, yielding

$$\frac{2}{f} - 1 + 0.207\frac{d_W}{a^*_B} = 4F(N_{sc}, f), \qquad (27)$$

where $F(N_{sc}, f)$ is the same as in equation (21), but g_1 now reads

$$g_1(N_{sc}, x, x', \varphi) = \left[\sqrt{\pi N_{sc}} a_B^* \times \sqrt{(x+x')^2 - 4xx' \sin^2\varphi} + f q_s^{(1)}/q_s^{(0)}\right]^{-1}. \quad (28)$$

The polarization-dependent effective-mass approximation does not change the previous result regarding the monotonically decreasing dependence of N_{sc} on d_W since $f < 1$. We show that the solutions of the approximate (in the sense that it contains some approximations beyond our basic scheme, described in Sect. 2.3) equation (27) (dashed curve) depicted in Figure 2 for $f = 0.65$, fit precisely the original values (open squares). We observe that since $F(0, f) = \frac{1}{4}(\frac{2}{f} - \frac{1}{2})$, d_{WL} does not depend on f (see Eq. (27)). Thus, d_{WL} depends on correlations, in our Thomas-Fermi model, via the ratio $q_s^{(0)}/q_s^{(1)}$ and, consequently, the relation $d_{WL} = 2.42 a_B^*$ is universal in the sense that it is valid for all materials (the material determines the value of a_B^*). We note that this result does not depend on the approximations made to derive equation (27) since those approximations become immaterial as N_s tends to zero.

Up (down) triangles in Figure 4 correspond to *infinite* (*finite*) QWs where we have taken the ratio f as the dashed curve in the inset of Figure 3 (Attaccalite et al. [4]). We note that the MC density interval for spontaneous spin polarization mentioned in Section 1, appears notoriously shrunk for the *finite* QWs studied here. In fact, from Figure 4 we obtain a new density interval for the transition densities in *finite* QWs between $N_{sc} = 3.2 \times 10^7$ cm^{-2} and $N_{sc} = 6.1 \times 10^8$ cm^{-2}. We take these values from the transition densities at the maximum of the curves related to FN-DMC (down triangles) and VMC (open circles) respectively.

4 Discussion

In reference [14], the spin susceptibility ($= m^* g^*$) has been measured in a high quality 200-fold GaAs/AlGaAs superlattice of 100 Å of GaAs wells and 30 Å barriers of $Al_{0.32}Ga_{0.68}As$, with unprecedented low densities such as $N_s = 1.7 \times 10^9$ cm^{-2} ($r_s = 13.9$) and no transition was observed. According to what we have mentioned above, this is not surprising. There are several possible reasons for this negative result. We first note that the density used, although low enough for a transition in the pure 2DEG, is clearly too high considering the finite well width for *finite* QWs: for $d_W = 100$ Å (Fig. 4), the electron density achieved in reference [14] is 6.5 times higher than our critical density (open circles) which uses the ratio f that matches the 2DEG value from reference [2] and 50 times higher than the critical density (down triangles) which uses the r_s-dependent ratio f that matches the 2DEG energy shifts E_{shift} from reference [4]. Also, due to the tunneling of the electrons into the AlGaAs barriers, the superlattice acts like a single, extremely wide QW. Furthermore, it is possible that if the QW were sufficiently wide, the quasi-2DEG could lose its two-dimensional characteristics, allowing for stable partially-polarized phases like those possible in the 3DEG, turning more difficult the detection of the transition. We note that the effects of in-plane correlations combined with the finite well widths and heights of QWs produce a drastic diminution of the transition densities by a factor that ranges from 3 to 15 depending on which method VMC or FN-DMC turns out to be the best tool to estimate the transition density in pure 2DEG. For the best case, it should become necessary to achieve electron densities lower that the ones studied experimentally thus far by a factor of 3 and by a factor of 53 in the worst case. Very different could be the quasi-two-dimensional hole gas (quasi-2DHG) scenario since in that system, high r_s values such as $r_s \approx 80$ are already attainable [24]. However, our theoretical predictions about the critical transition density in n-doped GaAs/AlGaAs QWs cannot be straightforwardly translated to quasi-2DHG. The adaptation of our formalism to the problem with holes is currently in progress.

Based on the insight gained from our calculations, we propose that the optimal conditions for observing a ferromagnetic transition in multiple QWs are:
(a) well widths between 30 Å and 50 Å
(b) wide AlGaAs barriers between wells to prevent tunneling, and
(c) well height V_b as large as possible to minimize barrier-penetration effects.

In a recent experimental work, Gosh et al. [25] report a possible spontaneous spin polarization in mesoscopic two-dimensional systems that is at odds with our findings. They have used 2DEGs in Si δ-doped GaAs/AlGaAs heterostructures with densities as low as $N_s = 5 \times 10^9$ cm^{-2} ($r_s = 7.6$) and the temperature was set at $T = 40$ mK or equivalently $T/T_F \approx 0.02$ since $T_F = 2.3$ K at $r_s = 7.6$. Somewhat surprisingly, according to their interpretation of the data, these authors found partial spin polarization with $\zeta = 0.2$. The authors attribute this partial spin polarization to the finite T since no partial spin polarization is possible in 2DEG at $T = 0$ [4,16]. However, in reference [16] the authors find partial spin polarization for T/T_F between 0.3 and 1.6, i.e. well above $T/T_F = 0.02$ reported in reference [25]. On the other hand, $r_s = 7.6$ is considerably lower than the lowest value for spin polarization in 2DEG [2].

5 Summary

In summary, we have calculated the ferromagnetic critical density at $T = 0$ of the quasi-two-dimensional electron gas confined in semiconductor GaAs-based symmetrically-doped quantum wells. We use the screened Hartree-Fock approximation to which we add different effective masses for both spin polarizations in order to take into account Coulomb correlations beyond screening.

Once the value of the effective mass for the polarized phase is adjusted so as to reproduce the transition density

for the pure 2D case calculated with the VMC method, our theory gives ground-state energy shifts that agree with those of VMC. On the other hand, a density-dependent ratio between both effective masses is required to fit the ground-state energy shifts calculated with the FN-DMC method.

We predict that, for QWs with only one occupied subband, there is a maximum well width beyond which the polarized state would be energetically unfavorable at all densities.

Based on our theory and the existing MC calculations for the 2DEG, we predict that narrow quantum wells (with well widths roughly in the range 30 Å $\leq d_W \leq$ 50 Å) should exhibit a ferromagnetic transition at a density range between $N_{sc} = 3.2 \times 10^7$ cm^{-2} ($r_s \approx 100$) and $N_{sc} = 6.1 \times 10^8$ cm^{-2} ($r_s \approx 23$). This range, which looks far from the densities achievable nowadays in GaAs quasi-2DEG, is, on the other hand, already within reach in GaAs quasi-2DHG systems.

The authors acknowledge partial support from Proyectos UBA-CyT 2001-2003 and 2004-2007, ANPCyT project PICT 03-11609, and Fundación Antorchas. P.I.T. is a researcher of CONICET.

References

1. F. Bloch, Z. Phys. **57**, 545 (1929)
2. D. Ceperley, Phys. Rev. B **18**, 3126 (1978)
3. B. Tanatar, D.M. Ceperley, Phys. Rev. B **39**, 5005 (1989)
4. C. Attaccalite, S. Moroni, P. Gori-Giorgi, G.B. Bachelet, Phys. Rev. Lett. **88**, 256601 (2002)
5. G. Ortiz, M. Harris, P. Ballone, Phys. Rev. Lett. **82**, 5317 (1999)
6. W.M.C. Foulkes, L. Mitas, R.J. Needs, G. Rajagopal, Rev. Mod. Phys. **73**, 33 (2001)
7. Y. Kwon, D.M. Ceperley, R.M. Martin, Phys. Rev. B **48**, 12037 (1993)
8. T. Ando, A.B. Fowler, F. Stern, Rev. Mod. Phys. **54**, 437 (1982)
9. J.H. Davies, *The Physics of Low-Dimensional Semiconductors* (Cambridge University Press, New York, 1998)
10. F.T. Vasko, A.V. Kuznetsov, *Electronic States and Optical Transitions in Semiconductor Heterostructures* (Springer-Verlag, New York, 1999)
11. G. Bastard, *Wave Mechanics Applied to Semiconductor Heterostructures* (Halsted Press, New York, 1988)
12. H. Haug, S.W. Koch, *Quantum Theory of the Optical and Electronic Properties of Semiconductor*, 2nd edn. (World Scientific, Singapore, 1993), Chap. 7
13. R.J. Radtke, P. I. Tamborenea, S. Das Sarma, Phys. Rev. B **54**, 13832 (1996)
14. J. Zhu, H.L. Stormer, L.N. Pfeiffer, K.W. Baldwin, K.W. West, Phys. Rev. Lett. **90**, 056805 (2003)
15. M.S.C. Luo, S.L. Chuang, S. Schmitt-Rink, A. Pinczuk, Phys. Rev. B **48**, 11086 (1993)
16. M.W.C. Dharma-wardana, F. Perrot, Phys. Rev. Lett. **90**, 136601 (2003)
17. We observe a missing factor 4π in equations (12), (13) and (14) of reference [15] and an incorrect k factor in equation (14)
18. A. Manolescu, R.R. Gerhardts, Phys. Rev. B **56**, 9707 (1997)
19. A.L. Fetter, J.D. Walecka, *Quantum Theory of Many-Particle Systems* (McGraw-Hill, Boston, 1971)
20. A.K. Rajagopal, J.C. Kimball, Phys. Rev. B **15**, 2819 (1977)
21. E. Tutuc, S. Melinte, E.P. De Poortere, M. Shayegan, R. Winkler, Phys. Rev. B **67**, 241309(R) (2003)
22. Y.-R. Jang, B.I. Min, Phys. Rev. B **48**, 1914 (1993)
23. A. Krakovsky, J.K. Percus, Phys. Rev. B **53**, 7352 (1996)
24. H. Noh, M.P. Lilly, D.C. Tsui, J.A. Simmons, E.H. Hwang, S. Das Sarma, L.N. Pfeiffer, K.W. West, Phys. Rev. B **68**, 165308 (2003)
25. A. Ghosh, C.J.B. Ford, M. Pepper, H.E. Beere, D.A. Ritchie, Phys. Rev. Lett. **92**, 116601 (2004)